Synergistic Antitumor Effects of Transarterial Viroembolization for Multifocal Hepatocellular Carcinoma in Rats

Jennifer Altomonte,[1] Rickmer Braren,[2] Stephan Schulz,[3] Sabrina Marozin,[1] Ernst J. Rummeny,[2] Roland M. Schmid,[1] and Oliver Ebert[1]

Oncolytic virotherapy is a promising strategy for safe and effective treatment of malignancy. We have reported previously that recombinant vesicular stomatitis virus (VSV) vectors are effective oncolytic agents that can be safely administered via the hepatic artery in immunocompetent rats to treat multifocal hepatocellular carcinoma (HCC), resulting in tumor necrosis and prolonged survival. Though the results were encouraging, complete tumor regression was not observed, which led us to explore alternative approaches to further enhance the efficacy of VSV treatment. Transarterial embolization techniques have been shown to improve the efficiency and tumor selectivity of anticancer treatments. Degradable starch microspheres (DSM) are one such embolic agent that provides transient embolization of the therapeautic agent before being degraded by serum amylases. Here we demonstrate via dynamic contrast-enhanced magnetic resonance imaging that in our rat model of multifocal HCC, DSM injection into the hepatic artery results in a substantial reduction in tumor perfusion of systemically applied contrast agent. VSV, when administered in combination with DSM, results in enhanced tumor necrosis and synergistically prolongs survival when compared with VSV or DSM monotherapy. *Conclusion:* This regimen of viroembolization represents an innovative therapeutic modality that can augment the future development of transarterial oncolytic virus therapy for patients with advanced HCC. (HEPATOLOGY 2008;48: 1864-1873.)

Hepatocellular carcinoma (HCC) represents a major worldwide health concern, ranking among the top five most prevalent malignancies.[1] The incidence of HCC has more than doubled over the last two decades,[2] and now accounts for over 500,000 new cases annually.[3-5] Recent reports suggest that the rate of HCC diagnoses will continue to rise, presumably as a consequence of an ever-increasing prevalence of hepatitis C virus infection and increased alcohol consumption observed in most industrialized countries.[6,7]

Whereas the incidence of HCC has been increasing steadily, the emergence of new and effective therapeutic agents remains relatively stagnant. The majority of HCC cases are detected at an advanced stage, at which time the treatment options are even further limited.[5] Surgical resection and liver transplantation are considered curative; however, the majority of patients do not meet the strict criteria designated by such treatments. In general, surgical therapy is indicated only in patients with limited HCC progression (1 to 3 nodules), without portal hypertension or advanced underlying liver disease.[8,9] The feasibility of liver transplantation is further limited by a shortage of donor livers, resulting in waiting times in excess of 12 months in some Western countries.[10]

For patients with nonresectable HCC or patients on the waiting list for liver transplantation, local regional therapy using transarterial embolization (TAE) or transarterial chemoembolization (TACE) are considered stan-

Abbreviations: DCE-MRI, dynamic contrast-enhanced magnetic resonance imaging; DSM, degradable starch microspheres; HCC, hepatocellular carcinoma; MTS, 3-(4,5-dimethylthiazol-2-yl)-5-(3-carboxymethoxyphenyl)-2-(4-sulfophenyl)-2H-tetrazolium; NK, natural killer; PBS, phosphate-buffered saline; pfu, plaque-forming units; TACE, transarterial chemoembolization; TAE, transarterial embolization; TCID50, tissue culture infectious dose 50; VSV, vesicular stomatitis virus.

From [1]II. Medical Clinic, [2]Institute for Radiology, and [3]Institute for Pathology, Technical University of Munich, Munich, Germany.

Received March 7, 2008; accepted July 20, 2008.

Supported in part by the German Research Aid (Max-Eder Research Program) and the Federal Ministry of Education and Research (Grant 01GU0505).

Address reprint requests to: Oliver Ebert, II Medizinische Klinik und Poliklinik, Klinikum rechts der Isar, Technical University of Munich, Trogerstr. 32, 81675 Munich, Germany. Email: oliver.ebert@lrz.tum.de; fax: (49)-89-41402258.

Published online in Wiley InterScience (www.interscience.wiley.com).

DOI 10.1002/hep.22546

Potential conflict of interest: Nothing to report.

dard palliative treatment.[11-13] The rationale for such therapies lies in the dual blood supply feeding the liver. Whereas normal hepatocytes receive the majority of their blood flow from the portal vein, with only about 25% being supplied by the hepatic artery, tumors receive their blood almost exclusively from the hepatic artery.[14] TAE and TACE therapies exploit this unique feature by blocking the arterial blood flow in the liver, thereby delivering a concentrated dose of a chemotherapeutic drug and/or embolizing agent selectively to the tumor, resulting in ischemia-induced necrosis and enhanced oncolysis due to a prolonged exposure time of the tumor cells to the chemotherapeutic agent.[15,16] Although it is generally accepted that TAE and TACE techniques result in substantial tumor response after treatment,[17,18] several trials have produced controversial data regarding a resulting prolongation of survival.[19-21] Furthermore, it is not yet clear whether the incorporation of chemotherapy provides an additional survival benefit over TAE alone.

Due to the overwhelming deficit in effective treatment options for HCC, several alternative approaches have emerged. Oncolytic viruses are a promising option due to their intrinsic ability to selectively replicate and kill tumor cells while sparing the surrounding normal tissue.[22-24] Vesicular stomatitis virus (VSV), a negative-strand RNA virus of the *Rhabdoviridae* family, is a particularly appealing oncolytic vector because of its wide host range, short replication cycle, and ability to reach high titers in many rodent and human tumor cell lines. VSV is nonpathogenic in humans and derives its tumor selective replication through its extreme sensitivity to the antiviral effects of type I interferon responses in normal cells, which are defective in most tumor cells.[25] Furthermore, because the general population has never been exposed to VSV, it is presumed that there will be no issue of pre-existing immunity, which would interfere with its future potential for clinical application.[26]

We have previously described the efficacy of recombinant VSV vectors as oncolytic agents for treatment of orthotopic HCC in immunocompetent rats.[27] We demonstrated that, by vector infusion through the hepatic artery, VSV could effectively gain access and selectively replicate in multifocal HCC tumors of various sizes, resulting in tumor necrosis and prolongation of survival.[28-30] Though these results are encouraging, complete tumor regression was not achieved, and the remaining viable tumor eventually relapsed, preventing the possibility of long-term survival. Based on these observations, we sought an alternate strategy to improve upon the outcome of VSV therapy for HCC.

We present a therapeutic approach for the treatment of multifocal HCC, involving recombinant VSV administered in combination with an embolization agent, and infused through the hepatic artery in tumor-bearing rats. In this study, we used degradable starch microspheres (DSM), an embolic agent currently being used clinically for TAE of HCC and metastatic liver tumors, injected as a mixture with a low dose of our previously reported rVSV-F vector. This strategy, which we have termed viroembolization, resulted in massive tumor necrosis and translated to substantial prolongation of survival in comparison to monotherapy with either VSV or DSM alone.

Materials and Methods

Cell Lines. The rat HCC cell line McA-RH7777 was purchased from the American Type Culture Collection (Manassas, VA) and maintained in Dulbecco's modified Eagle's medium adjusted to contain 1.5 g/L sodium bicarbonate and 4.5 g/L glucose (American Type Culture Collection). BHK-21 cells purchased from the American Type Culture Collection were maintained in Glasgow minimum essential medium (GIBCO, Carlsbad, CA). All culture media were supplemented with 10% heat-inactivated fetal bovine serum (Biochrome, Berlin, Germany), and all cells were cultured in a humidified atmosphere at 5% CO_2 and 37°C.

Recombinant Virus. The construction and rescue of the rVSV vector expressing a mutant (L289A) NDV fusion protein (rVSV-F) has been described.[28] The virus was amplified on BHK-21 cells, and the supernatant was purified with a sucrose gradient. Briefly, the cells were infected at a multiplicity of infection of 0.0001, and 48 hours later, the supernatant was collected and centrifuged to clear floating cells. The supernatant was then subjected to ultra-centrifugation at 24,000 rpm for 1 hour. The pellet was resuspended in phosphate-buffered saline (PBS) and layered on top of a sucrose gradient ranging from 60% to 10%, and ultra-centrifuged for 1 hour at 24,000 rpm. The band containing the virus was carefully collected with a syringe and 20-gauge needle, aliquoted, and stored at −80°C.

Growth Curves. Viral growth in the presence and absence of degradable starch microspheres (EmboCept, PharmaCept, Berlin, Germany) was compared in McA-RH7777 cells. The cells were plated in 6-well dishes at 1×10^6 cells per well, and infected with rVSV-F at a multiplicity of infection of 10, mixed with an equal volume of either DSM or PBS in triplicate. After infection at room temperature for 30 minutes, cells were washed three times with PBS, and fresh complete medium was added. Aliquots of supernatant were collected at 0, 8, 16, and 24 hours postinfection, and assayed for viral titer via tissue culture infectious dose 50 (TCID50) analysis.

Cell Proliferation Assay. McA-RH7777 cells were seeded overnight in 24-well dishes at 2×10^5 cells per well and infected the following day with rVSV-F at a multiplicity of infection of 10, mixed with an equal volume of either DSM or PBS. Cell viability was measured at 0, 6, 12, 24, 48, and 72 hours after infection using the 3-(4,5-dimethylthiazol-2-yl)-5-(3-carboxymethoxyphenyl)-2-(4-sulfophenyl)-2H-tetrazolium (MTS) tetrazolium compound (CellTiter96 AQ_{ueous} One Solution Cell Proliferation Assay, Promega, Madison, WI). All cell viability data are expressed as a percentage of viable cells compared withmock-infected controls at each time point.

Animal Studies. All procedures involving animals were approved and performed according to the guidelines of the institution's animal care and use committee and the government of Bavaria, Germany. Six-week-old male Buffalo rats were purchased from Harlan Winkelmann (Borchen, Germany), and housed under standard conditions. To establish multifocal HCC lesions within the liver, 10^7 syngeneic McA-RH7777 rat HCC cells were infused as a 1-mL suspension in serum-free Dulbecco's modified Eagle's medium through the portal vein. A second laparotomy was performed 21 days after tumor cell implantation, and animals with visible tumors within the range of 1 to 10 mm in diameter were randomly assigned to the following treatment groups: PBS, DSM, rVSV-F, or combination treatment of rVSV-F plus DSM. All treatments were administered as a 1-mL solution injected via the hepatic artery. A dose of 1×10^6 plaque-forming units (pfu) of VSV was used in the monotherapy and combination group. 500 μL of DSM was diluted 1:1 with either PBS or rVSV-F, depending on the treatment group. Representative animals from each group were sacrificed on day 1 and day 3 for histology and immunohistochemical analysis of tumor and liver sections. In addition, TCID50 analysis of extracts from snap-frozen tumor samples was performed for quantification of VSV yield on day 1. Finally, animals were followed for survival to compare the therapeutic outcome of each treatment. The animals were monitored daily and euthanized at humane endpoints.

Magnetic Resonance Imaging Acquisition and Image Analysis. Magnetic resonance images were acquired on a 1.5-T whole-body magnetic resonance imaging scanner (Philips, Achieva, Netherlands). Buffalo rats bearing multifocal McA-RH7777 HCC tumors, either untreated or treated with transarterial injection of DSM, were subjected to dynamic contrast-enhanced magnetic resonance imaging (DCE-MRI) approximately 30 minutes after infusion of the embolization agent. Rat livers were imaged individually using a 47-mm surface coil (Philips). Axial images were obtained for tumor localization using a T1-weighed three-dimensional gradient echo sequence (Repetition Time [TR] = 20 ms, Echo Time [TE] = 4.6 ms, flip angle = 30°, Field of View [FOV] = 6.4 × 4.0 cm, imaging matrix = 224 × 179, slice thickness = 1 mm). Contrast dynamics with three baseline scans and 27 postcontrast scans were then visualized using an axial T1-weighted three-dimensional gradient echo sequence (TR = 20 ms, TE = 2.9 ms, flip angle = 45° slice thickness = 2 mm) with a time resolution of 28 seonds/dynamic. Bolus injection via the tail vein of 0.2 mmol/kg GdDTPA (Magnevist, Bayer HealthCare Pharmaceuticals) was performed manually within 2 seconds. Data were quantitatively analyzed using View Forum software (Philips, Netherlands) by measuring gray-scale signal intensities in equally sized regions of interest within tumor nodules and adjacent normal liver tissue.

Histology and Immunohistochemistry. Liver sections containing tumor were fixed overnight in 4% paraformaldehyde and paraffin-embedded. Three-micrometer-thin sections were subjected to either hematoxylin-eosin staining for histological analysis or immunohistochemical staining using monoclonal antibodies against VSV/G protein (Alpha Diagnostic, San Antonio, TX), CD31 (Santa Cruz Biotechnology, Santa Cruz, CA), and natural killer (NK) cell marker ANK61 (Santa Cruz Biotechnology). Terminal deoxynucleotidyl transferase-mediated dUTP nick-end labeling was performed using the *In Situ* Cell Death Detection Kit, Flourescein (Roche, Indianapolis, IN) according to the manufacturer's protocol. ImageJ software (National Institutes of Health, Bethesda, MD) was used for morphometric analysis of tumors, and necrotic areas were measured and expressed as a percentage of the entire tumor area.

Statistical Analyses. For comparison of individual data points, a two-sided Student *t* test was applied to determine statistical significance. Survival curves were plotted according to the Kaplan-Meier method, and statistical significance between different treatment groups was determined using the log-rank test. Statistical data were obtained using GraphPad Prism 5.0 (GraphPad Software, San Diego, CA). *P* values of less than 0.05 were considered statistically significant.

Results

In Vitro *Characterization of DSM Treatment on HCC Cells.* To rule out an inhibitory effect of the embolization agent on viral replication, rVSV titers in McA-RH7777 cells were monitored in the presence versus absence of DSM. Aliquots of the supernatants were harvested at the indicated time points and subjected to TCID50 analysis, and the growth curves were plotted

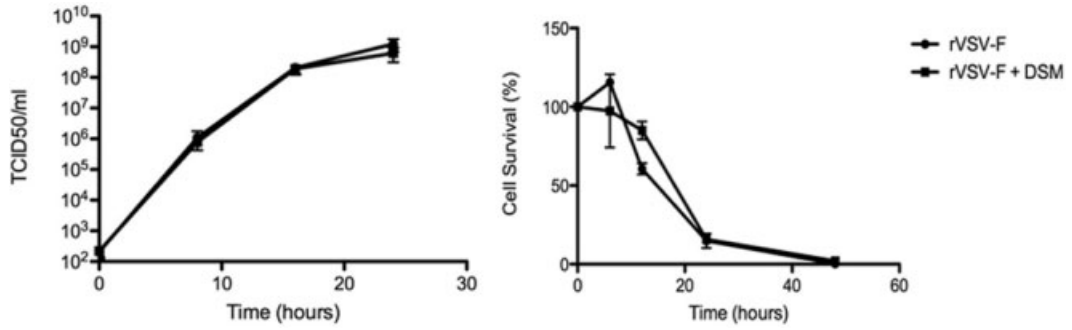

Fig. 1. DSM does not alter viral replication and cell killing of rVSV-F in McA-RH7777 rat HCC cells in vitro. Rat McA-RH7777 cells were infected at a multiplicity of infection of 10 in the presence or absence of degradable starch microspheres (DSM). Left: TCID50 assays were performed on conditioned media at 0, 8, 16, and 26 hours after infection. Right: MTS assays for cell viability were performed at 0, 6, 12, 24, 48, and 72 hours after infection. Triplicate samples were analyzed at each time point. Data are expressed as the mean ± standard deviation.

(Fig. 1). The virus replicated to similar titers at all time points tested, regardless of the presence of DSM during infection. Furthermore, to determine a cytotoxic effect incurred by DSM on VSV-infected McA-RH7777 cells, MTS assays were performed at various time points after treatment with rVSV alone or with rVSV plus DSM. The kinetics of cell killing in each group was nearly identical.

In Vivo Imaging of Embolized Tumors. To monitor the effectiveness of transarterial infusion of DSM in HCC tumor-bearing rats, animals were randomly assigned as untreated controls or treated with DSM via the hepatic artery. Approximately 30 minutes after embolization, the animals were subjected to DCE-MRI. Perfusion of the gadolinium contrast agent within the tumors and normal surrounding liver was analyzed (Fig. 2). The resulting intensity plots revealed perfusion of tumor and liver tissue with a prolonged washout phase in the tumor tissue compared with the normal liver tissue, while in the embolized animals only the normal liver tissue is perfused with contrast agent. These data indicate that hepatic arterial infusion of DSM results in nearly complete embolization of tumors, while having little effect on normal liver perfusion at early time points.

VSV/G Expression Within Tumors Treated by Viroembolization. To assess the in vivo effect of VSV administered in combination with an embolization agent, animals were randomly assigned to receive rVSV-F monotherapy or combination therapy of rVSV-F plus DSM. To compare the contents of VSV within tumor and normal liver tissues administered in the presence versus absence of embolization agent, three animals per group were sacrificed on day 1 after treatment for histo-

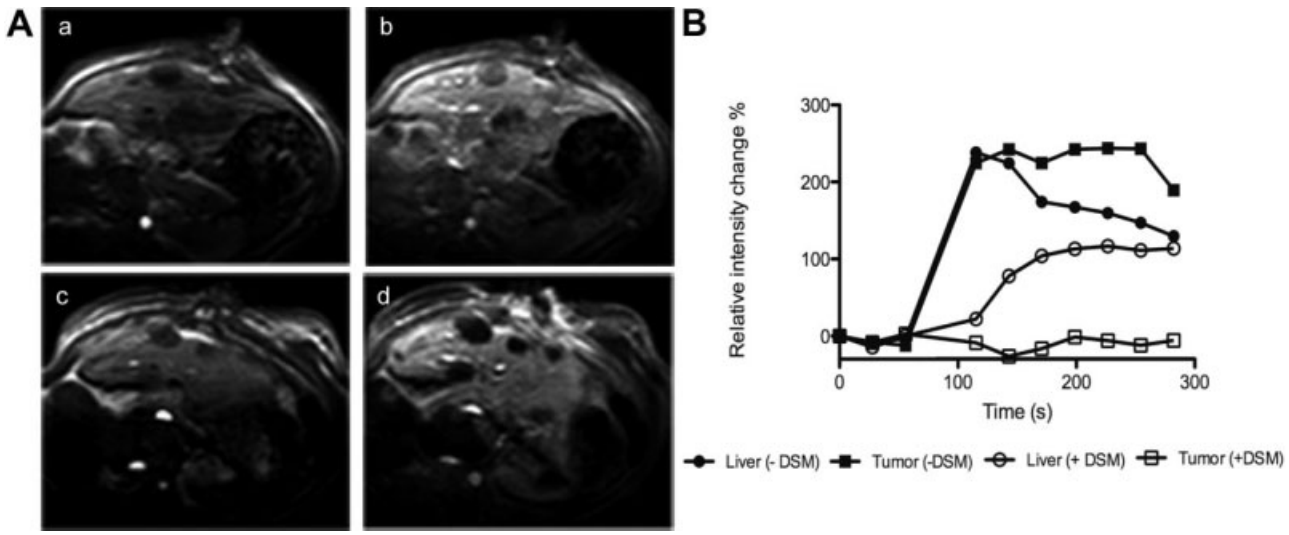

Fig. 2. Dynamic contrast-enhanced magnetic resonance imaging. McA-RH7777 tumor-bearing rats, either nonembolized or 30 minutes after hepatic arterial embolization with DSM, were imaged with DCE-MRI. (A) Axial T1-weighed precontrast (a, c) and postcontrast (b, d) images show lack of contrast in embolized tumor nodules (d). (B) Data were quantitatively analyzed by measuring gray-scale signal intensities in equal-sized regions of interest of tumor nodules and adjacent normal liver tissue. One representative data set is shown.

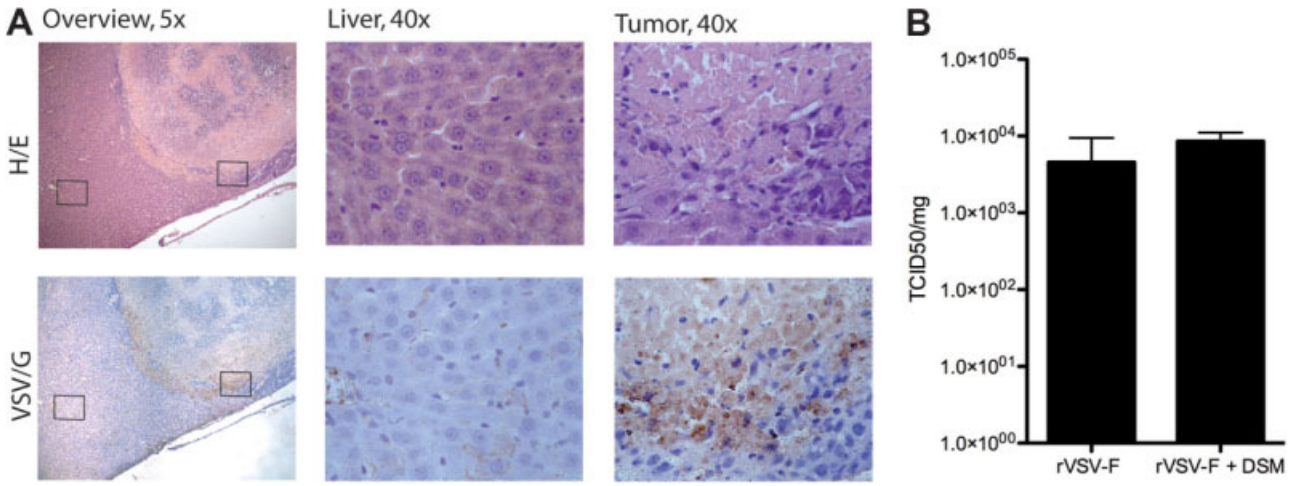

Fig. 3. Tumor-specific VSV/G expression localized in viable border region of HCC after treatment with rVSV-F and DSM. Tumor-bearing rats were treated via hepatic arterial infusion with PBS, DSM, rVSV-F, or DSM plus rVSV-F with a viral dose of 1×10^6 pfu/animal. Tumor samples were obtained on day 1 after treatment. (A) Three-micrometer-thin paraffin sections were stained with hematoxylin-eosin (upper panel) and a monoclonal anti-VSV/G antibody counterstained with hematoxylin (lower panel). Representative sections of liver and tumor are shown at low (×5) and high (×40) power. (B) Tumor samples were snap frozen, and lysates were subjected to TCID50 analysis to compare intratumoral virus titers in rVSV-F versus rVSV-F and DSM-treated rats. Results are expressed as the mean + standard deviation.

logical and immunohistochemical staining, as well as quantification of viral titers via TCID50 analysis (Fig. 3). Immunohistochemical staining using a monoclonal antibody against VSV/G revealed VSV/G protein localized within the viable tumor rim of viroembolized animals. Importantly, the histology of neighboring hepatic parenchyma in both treatment groups was completely normal, and in consecutive sections there was no evidence for VSV/G expression via immunohistochemistry (Fig. 3A). TCID50 analyses of snap-frozen tumor lysates demonstrated similar viral titers in the two groups (Fig. 3B). Infectious VSV particles within the normal liver were below the level of detection (10 pfu/mg wet weight) and subsequently could not be determined.

Enhanced Tumor Response in Viroembolized HCC Tumor-Bearing Rats. To determine the impact of transarterial viroembolization on tumor viability, multifocal HCC-bearing rats were treated with PBS, DSM, rVSV-F, or rVSV-F plus DSM and were euthanized on day 3 after treatment. Liver sections containing tumor were prepared for hematoxylin-eosin staining and analyzed morphometrically for quantification of necrotic areas (Fig. 4). ImageJ software was employed to measure necrotic areas, which were then calculated as a percentage of the entire tumor area. In the PBS control group, less than 15% necrosis was observed, which can be attributed to spontaneous necrosis that occurs naturally in most tumors. Whereas VSV treatment alone resulted in less than 30% necrosis, DSM treatment caused nearly 60% necrosis, and combination treatment resulted in more than 90% tumor necrosis. The morphometric analysis data are statistically significant for each group compared with every other group (that is, PBS versus rVSV-F, $P < 0.05$; DSM versus rVSV-F plus DSM, $P < 0.0001$).

Enhanced Apoptosis Observed in HCC Tumors Treated with rVSV-F. To identify a potential mechanism for the additive effect of rVSV-F plus DSM on tumor response, we compared the degree of apoptosis

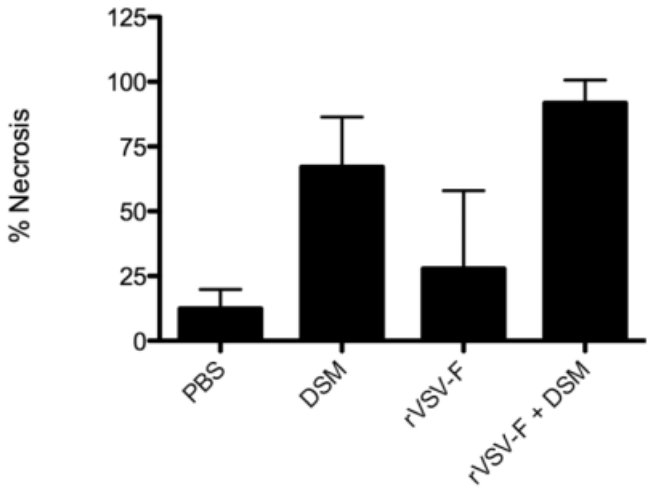

Fig. 4. Enhanced tumor response in multifocal HCC-bearing rats treated with rVSV-F and DSM. Rats bearing multifocal HCC tumors were infused via the hepatic artery with PBS, DSM, rVSV-F, or DSM plus rVSV-F with a viral dose of 1×10^6 pfu/animal, and sacrificed 3 days after treatment. Three-micrometer-thin tumor sections were stained with hematoxylin-eosin and analyzed. The percentage of necrotic area within each tumor was measured morphometrically using ImageJ software. Data are expressed as the mean + standard deviation, and the results were analyzed statistically via two-sided Student *t* test. All data were statistically significant compared with all other treatment groups ($P < 0.05$).

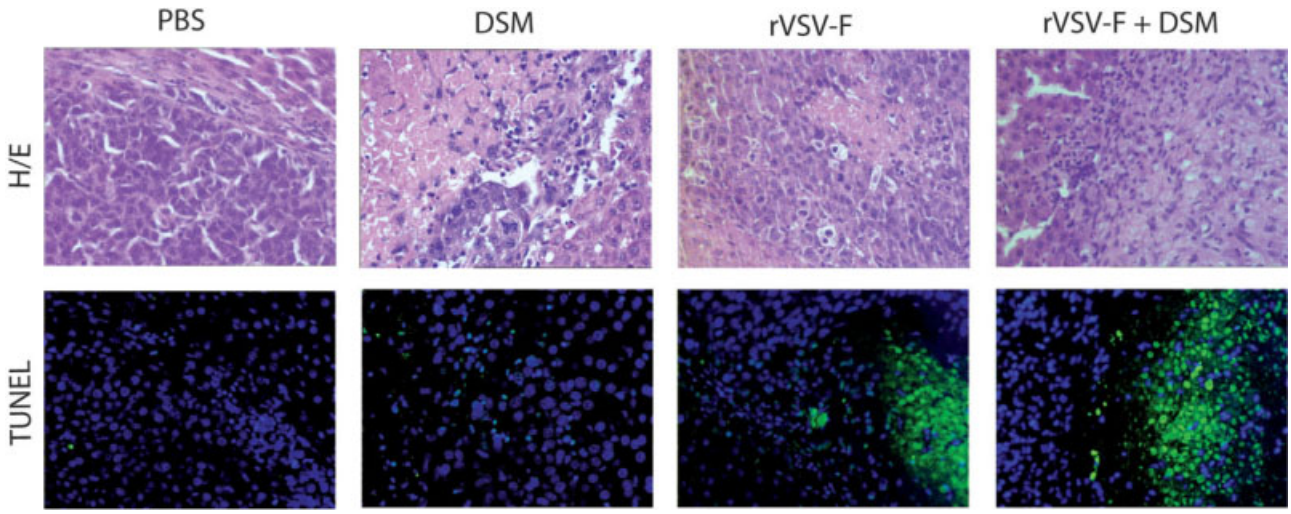

Fig. 5. Treatment with rVSV-F or viroembolization results in enhanced apoptosis in HCC tumors. Rats bearing multifocal HCC were treated via hepatic arterial infusion of PBS, DSM, rVSV-F, or DSM plus rVSV-F with a viral dose of 1×10^6 pfu/animal, and sacrificed 3 days after treatment. Three-micrometer-thin paraffin sections containing liver and tumor were subjected to hematoxylin-eosin analysis (top) or fluorescein-conjugated terminal deoxynucleotidyl transferase-mediated dUTP nick-end labeling and counterstained with 4',6-diamidino-2-phenylindole for localization of nuclei (bottom). Representative sections are shown (original magnification ×20).

among treatment groups. Although on day 1 there were no remarkable differences (data not shown), on day 3 we observed patches of apoptosis in tumors treated with rVSV-F alone, and significantly enhanced apoptosis in the outer borders of those tumors subjected to transarterial viroembolization (Fig. 5) compared with those treated with either monotherapy or PBS.

Attenuated CD31 Expression Following Treatment with rVSV-F. To investigate a possible anti-angiogenic effect of rVSV-F in HCC, we performed immunohistochemical analysis of CD31 in tumor sections on day 3 after treatment (Fig. 6, upper panel). Whereas normal vasculature with CD31+ endothelial staining was observed in tumors treated with PBS, rVSV-F and viroembolization resulted in almost complete loss of positive staining on vessel walls. In the DSM monotherapy group, we observed CD31 staining localized mainly to the border regions of tumors, indicating that the vasculature in this

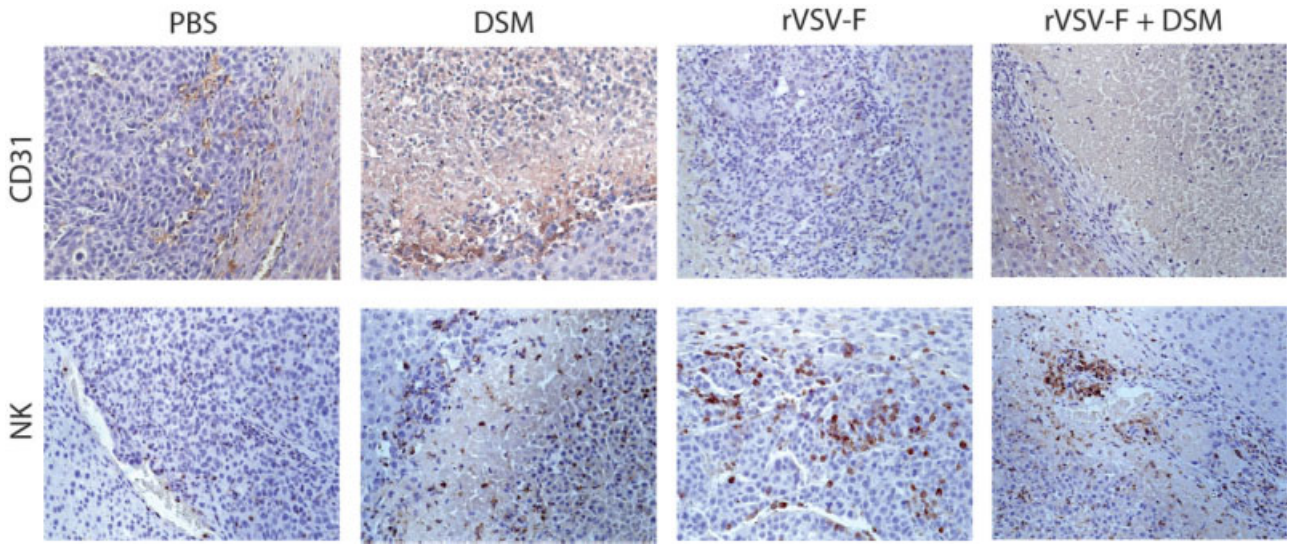

Fig. 6. rVSV-F causes reduction in CD31+ endothelial cells and stimulation of NK cell infiltration within tumors. Rats bearing multifocal HCC were treated via hepatic arterial infusion of PBS, DSM, rVSV-F, or DSM plus rVSV-F with a viral dose of 1×10^6 pfu/animal and sacrificed on day 3 after treatment. Three-micrometer-thin paraffin sections containing liver and tumor were analyzed via immunohistochemistry using a polyclonal antibody against CD31 (top) or NK cell marker ANK61 (bottom). Sections were counterstained with hematoxylin. Representative sections are shown (original magnification ×20).

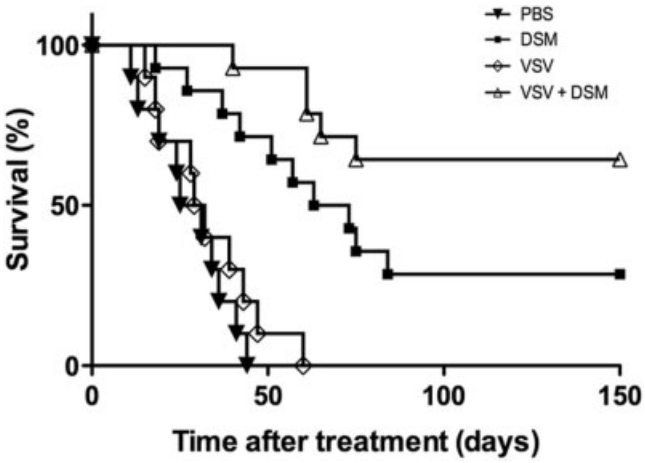

Fig. 7. DSM combined with rVSV-F results in significant survival prolongation in HCC-bearing rats. Multifocal hepatocellular carcinoma-bearing rats were treated with PBS (n = 10), DSM (n = 14), rVSV-F (n = 10), or DSM plus rVSV-F (n = 14) via hepatic arterial infusion and were followed for survival. Animals were monitored daily, and data were plotted as a Kaplan-Meier survival curve. Statistical significance was determined via log rank test.

area is still viable, and new angiogenesis has possibly been initiated.

Enhanced Infiltration of Inflammatory Cells in rVSV-F Infected Tumors. Because we postulated an inflammatory response conferred by the virus, we performed immunohistochmical staining of various immune cell markers on tumor tissue following treatment with PBS, DSM, rVSV-F, or rVSV-F plus DSM. Although we observed no significant differences in the numbers of macrophages and neutrophils among treatment groups (data not shown), we observed a significant infiltration of NK cells in tumors treated with virus, either alone or in combination with DSM (Fig. 6, bottom panel). To a lesser degree, DSM monotherapy also appeared to stimulate NK cell accumulation within tumors.

Significant Prolongation of Survival After Transarterial Viroembolization in Multifocal HCC-Bearing Rats. To assess the potential long-term benefit of the combination treatment modality for multifocal HCC tumor-bearing rats, a survival experiment was conducted. Tumor-bearing rats were randomly assigned to receive one of the following treatments via the hepatic artery: PBS (n = 10), DSM (n = 14), rVSV-F (n = 10), or DSM combined with rVSV-F (n = 14). Animals were monitored daily for survival, and the data were plotted as a Kaplan-Meier survival curve (Fig. 7). Although monotherapy with rVSV-F at this low dose did not significantly alter survival compared with PBS treatment, DSM treatment resulted in statistically significant survival benefit ($P < 0.0001$), both alone and in combination with rVSV-F. Furthermore, combination therapy with rVSV-F and DSM significantly prolonged survival compared with DSM treatment alone, resulting in more than 60% of viroembolized animals experiencing complete tumor regression. As dictated by Kaplan-Meier analysis, these data indicate a synergistic effect of the combination therapy. Furthermore, the long-term surviving rats were sacrificed after 150 days and evaluated for signs of residual malignancy. Macroscopically, there was no visible tumor within the liver or elsewhere, and there was no histological evidence of residual tumor cells or liver toxicity.

Discussion

Although oncolytic virus therapy represents a promising approach for treatment of multifocal cancers, it has several limitations. In our previous studies, we reported that VSV administration via the hepatic artery in HCC tumor-bearing rats results in tumor-selective viral replication and oncolysis[27-30]; however, intratumoral virus spread and treatment efficacy is limited, highlighting the need for an improved strategy. We report a treatment modality in which oncolytic VSV therapy was significantly enhanced by coadministration with a clinically approved embolization agent, which resulted in an impressive cure rate.

In this study, we used EmboCept, a representative of the group of embolization agents known as DSM. DSM are manufactured from hydrolyzed potato starch and provide relatively transient embolization before being degraded by serum amylases.[31] Although the physical presence of DSM within tumor vessels is temporary, the effect can be long-lasting due to the formation of emboli at the arterio-capillary level, as well as hypoxia and ischemic necrosis, which prevent reperfusion of the tumor.[32,33] After first confirming in vitro that DSM do not interfere or alter the ability of VSV to replicate in or kill tumor cells, our next major concern was the ability of DSM, when administered via the hepatic artery, to effectively embolize multifocal HCC lesions in our rat model. By performing DCE-MRI with embolized and nonembolized tumor-bearing rats, we were able to confirm that DSM resulted in complete embolization of all tumors analyzed, regardless of size. Furthermore, although there was a slight delay in gadolinium uptake in the livers of embolized animals, the peak was equivalent to that in the control animals, indicating that the embolic effect was tumor-specific.

It is well documented that the peripheral border of HCC lesions close to the surrounding nonneoplastic liver tissue has a tendency to survive TAE treatment, because this area is supplied by portal blood flow and collateral

circulation. Therefore, we hypothesized that transient TAE therapy for HCC could be significantly enhanced via coadministration of oncolytic VSV. We envisioned that extensive tumor necrosis could be induced through hypoxia and ischemia–reperfusion injury secondary to transient embolization, and the remaining viable rim could then be eradicated via VSV replication. Indeed, this is exactly what we observed through immunohistochemical analysis of VSV/G, which did in fact colocalize to the viable peripheral tumor regions. Although the number of recovered infectious viral particles, as determined by TCID50 analysis, was not significantly higher in the viroembolization group compared with VSV monotherapy, we speculated that this was due to the extent of tumor necrosis, which limited the areas where the virus could replicate to the border regions where viable tumor remained.

A comparison of the in vivo efficacy of transarterial viroembolization to each monotherapy revealed that, while VSV resulted in a modest effect, and embolization with DSM caused significantly enhanced tumor response, the most striking results were achieved by viroembolization, which resulted in more than 90% tumor necrosis. Impressively, we were able to achieve 60% long-term tumor-free survival through transarterial viroembolization of multifocal HCC in our rat model. Statistical analysis indicated that a synergistic effect was derived through combination of each monotherapy. These data clearly illustrated a superior effect of the combination treatment; however, it left open questions regarding the mechanism of the additive response. Because the effects of transarterial embolization in HCC have been fairly well characterized, we chose to focus on the contribution of VSV therapy to elucidate the mechanism whereby combination therapy confers its enhanced therapeutic outcome. In particular, we investigated the roles of apoptosis, antiangiogenesis, and inflammation as potential players.

VSV causes lysis of infected tumor cells through activation of apoptotic pathways, induced by expression of the viral matrix protein.[34,35] We hypothesized that VSV localized to the viable rim of tumors following embolization could induce apoptosis in the infected cells. Terminal deoxynucleotidyl transferase-mediated dUTP nick-end labeling revealed large areas of apoptosis in tumors treated with rVSV-F, whereas there was significantly less evidence of apoptosis in the PBS and DSM groups. Furthermore, apoptosis secondary to viroembolization was, in fact, mostly confined to the outer borders of the lesions, while in tumors treated with VSV monotherapy, it appeared in seemingly random patches, mainly in the core. Together, this implicated VSV induced-apoptosis as a contributing factor in eliminating the viable tumor rim, which survived embolization.

In addition to direct tumor cell lysis, it has been shown that VSV is also responsible for indirect killing of uninfected tumor cells through inhibition of vascular perfusion within infected tumors induced by the rapid recruitment of inflammatory cells to the tumor bed.[36] Furthermore, it was demonstrated that in situ expression of the VSV M protein resulted in decreased tumor vasculature in implanted glioma tumors in a rat model.[37] While embolization is known to stimulate angiogenesis,[38] in our model, we observed a clear reduction in CD31 staining within tumors treated in combination with VSV. The anti-angiogenic effect of VSV could provide a powerful tool for improving the efficacy of TAE by preventing new vessel formation feeding the remaining viable tumor cells.

In addition to the effect of inflammation on tumor blood flow, the infiltration of inflammatory cells in virus-infected tumor has the complimentary function of killing infected and surrounding tumor cells. The recruitment of NK cells to sites of VSV-infected tumor has been demonstrated,[39] and we have reproduced this phenomenon here. NK cells represent a distinct population of cytotoxic lymphocytes that act as an integral component of the innate cellular immune response system to invading viruses, prior to the launch of the adaptive immune responses.[40] These cells function by directly killing infected cells and inducing antiviral cytokines, and can result in a bystander effect by killing neighboring uninfected cells. Interestingly, several groups have recently attempted to combine TAE with adoptive immunotherapy in the clinic, and have shown enhancement of efficacy in patients.[41,42] In addition, oncolytic virus therapy may also promote cross-presentation of released tumor antigens to CD8+ T cells, leading to a long-term antitumor effect long after the virus is cleared.[43,44] Therefore, it is possible that long-term survival in the current study may be mediated by a tumor immune response, which is elicited through viral infection and oncolysis of the HCC cells.

Although we have not yet performed a direct comparison between TACE and viroembolization, several key factors indicate that viroembolization with VSV vectors might be the more effective therapy. Whereas a recent clinical report confirmed that TACE prolongs survival,[45] a comparison of TACE versus TAE alone demonstrated no survival difference.[46] This phenomenon can be explained by the well-documented fact that many HCCs are resistant to chemotherapeutic drugs,[47,48] which would support the concept that embolization is the more important component of TACE than chemotherapy. In addition, it has also been shown that hypoxia can further contribute to drug-resistance of cancer cells.[49] Because

TAE blocks arterial blood flow to the tumor, and subsequently results in hypoxia, it would follow that the efficacy of a chemotherapeutic drug might be further limited in this scenerio. In contrast, VSV has an inherent capacity for infecting and killing hypoxic cancer cells.[50] This ability could represent a critical advantage over existing therapies in treating established tumors.

In conclusion, this study has provided conclusive data to support the concept of viroembolization therapy for multifocal HCC. This is an innovative and effective treatment modality that results in massive tumor necrosis and extensive prolongation of survival compared with VSV or DSM monotherapy. Furthermore, through combination of VSV with a transient embolization agent, we were able to achieve enhanced efficacy despite administration of virus at 10-fold lower than the maximum tolerated dose, thereby improving the therapeutic index of viral therapy. Thus, viral therapy in combination with clinically approved embolization agents has the potential for providing potent oncolytic therapy for HCC and, potentially, metastatic liver tumors in cancer patients.

Acknowledgment: We thank PharmaCept GmbH (Berlin, Germany) for generously providing the EmboCept used in the study. In addition, we thank Barbara Lindner and Marcel Lee for excellent technical support.

References

1. Parkin DM, Bray F, Ferlay J.,Pisani, P. Estimating the world cancer burden: Globocan 2000. Int J Cancer 2001;94:153-156.
2. El-Serag HB, Mason AC. Rising incidence of hepatocellular carcinoma in the United States. N Engl J Med 1999;340:745-750.
3. Befeler A, Di Bisceglie AM. Hepatocellular carcinoma: diagnosis and treatment. Gastroenterology 2002;122:1609-1619.
4. Schafer DF, Sorrell MF. Hepatocellular carcinoma. Lancet 1999;353: 1253-1257.
5. Llovet J, Burroughs A, Bruix J. Hepatocellular carcinoma. Lancet 2003; 362:1907-1917.
6. Deuffic S, Poynard T, Buffat L, Valleron A-J. Trends in primary liver cancer. Lancet 1998;351:214-215.
7. Taylor-Robinson S, Foster GR, Arora S, Hargreaves S, Thomas HC. Increase in primary liver cancer in the UK. Lancet 1997;350:1142-1143.
8. Llovet J, Fuster J, Bruix J. Intention-to-treat analysis of surgical treatment for early hepatocellular carcinoma: resection versus transplantation. HEPATOLOGY 1999;39:1434-1440.
9. Bruix J, Castells A, Bosch J, Feu F, Fuster J, Garcia-Pagan JC, et al. Surgical resection of hepatocellular carcinoma in cirrhotic patients: prognostic value of preoperative portal pressure. Gastroenterology 1996;111:1018-1022.
10. Yao F, Bass NM, Nikolai B, Davern TJ, Kerlan R, Wu V, et al. Liver transplantation for hepatocellular carcinoma: analysis of survival according to the intention-to-treat principle and dropout from the waiting list. Liver Transpl 2002;8:873-883.
11. Blum H. Hepatocellular carcinoma: therapy and prevention. World J Gastroenterol 2005;11:7391-7400.
12. Bruix J, Sala M, Llovet JM. Chemoembolization for hepatocellular carcinoma. Gastroenterology 2004;127:S179-S188.
13. Miraglia R, Pietrosi G, Maruzzelli L, Petridis I, Caruso S, Marrone G, et al. Efficacy of transcatheter embolization/chemoembolization (TAE/TACE) for the treatment of single hepatocellular carcinoma. World J Gastroenterol 2007;13:2952-2955.
14. Lein W, Ackerman NB. The blood supply of experimental liver metastases. Surgery 1970;68:334-340.
15. Anderson J, Gianturco C, Wallace S. Experimental transcatheter intraarterial infusion-occlusion chemotherapy. Invest Radiol 1981;16:496-500.
16. Tancredi T, McCuskey PA, Kan Z, Wallace S. Changes in rat liver microcirculation after experimental hepatic arterial embolization: comparison of different embolic agents. Radiology 1999;211:177-181.
17. Llovet J, Bruix J. Systematic review of randomized trials for unresectable hepatocellular carcinoma: chemoembolization improves survival. HEPATOLOGY 2003;37:429-442.
18. Chang J, Tzeng WS, Pan HB, Yang CF, Lai KH. Transcatheter arterial embolization with or without cisplatin treatment of hepatocellular carcinoma: a randomized controlled study. Cancer 1994;74:2449-2453.
19. Bruix J, Llovet JM, Castells A, Montaua X, Bru C, Ayuso MC, et al. Transarterial embolization versus symptomatic treatment in patients with advanced hepatocellular carcinoma: results of a randomized controlled trial in a single institution. HEPATOLOGY 1998;27:1578-1583.
20. Pelletier G, Ducreux M, Gay F, Luboinski M, Hagege M, Dao T, et al. Treatment of unresectable hepatocellular carcinoma with lipiodol chemoembolization: a multicenter randomized trial. J Hepatol 1998;29:129-134.
21. Camma C, Schepis F, Orlando A, Albanese M, Shahied L, Trevisani F, et al. Transarterial chemoembolization for unresectable hepatocellular carcinoma: meta-analysis of randomized controlled trials. Radiology 2002;224: 47-54.
22. Kirn D, Martuza RL, Zwiebel J. Replication-selective virotherapy for cancer: biological principles, risk management, and future directions. Nat Med 2001;7:781-787.
23. Lorence RM, Katubig BB, Reichard KW, Reyes HM, Phuangsab A, Sassetti MD, et al. Complete regression of human fibrosarcoma xenografts after local Newcastle disease virus therapy. Cancer Research 1994;54: 6017-6021.
24. Peng KW, Ahmann GJ, Pham L, Greipp PR, Cattaneo R, Russell SJ, et al. Systemic therapy of myeloma xenografts by an attenuated measles virus. Blood 2001;98:2002-2007.
25. Stojdl DF, Lichty B, Knowles S, Marius R, Atkins H, Sonenberg N, Bell, JC. Exploiting tumor-specific defects in the interferon pathway with a previously unknown oncolytic virus. Nat Med 2000;6:821-825.
26. Rose JK, Whitt MA. Rhabdoviridae: the viruses and their replication. In: Knipe DM, Howley PM, eds. Fields Virology. 4th ed. Philadelphia: Lippincott Williams & Wilkins, 2001:1221-1242.
27. Ebert O, Shinozaki K, Huang TG, Savontaus MJ, Garcia-Sastre A, Woo SLC. Oncolytic vesicular stomatitis virus for treatment of orthotopic hepatocellular carcinoma in immune-competent rats. Cancer Res 2003;63: 611-613.
28. Ebert O, Shinozaki K, Kournioti C, Park MS, Garcia-Sastre A, Woo SL, et al. Syncytia induction enhances the oncolytic potential of vesicular stomatitis virus in virotherapy for cancer. Cancer Res 2004;64:3265-3270.
29. Shinozaki K, Ebert O, Kournioti C, Tai YS, Woo SL. Oncolysis of multifocal hepatocellular carcinoma in the rat liver by hepatic artery infusion of vesicular stomatitis virus. Mol Ther 2004;9:368-376.
30. Shinozaki K, Ebert O, Woo SL. Eradication of advanced hepatocellular carcinoma in rats via repeated hepatic arterial infusions of recombinant VSV. HEPATOLOGY 2005;41:196-203.
31. Erichsen C, Bolmsjo M, Hugander A, Jonsson PE. Blockage of the hepatic-artery blood flow by biodegradable microspheres (Spherex) combined with local hyperthermia in the treatment of experimental liver tumors in rats. Clin Oncol 1985;109:38-41.
32. Wang J, Murata S, Kumazaki T. Liver microcirculation after hepatic artery embolization with degradable starch microspheres. World J Gastroenterol 2006;12:4214-4218.
33. Yoshikawa T, Kokura S, Oyamada H, Iinuma S, Nishimura S, Kaneko T, et al. Antitumor effect of ischemia-reperfusion injury induced by transient embolization. Cancer Res 1994;54:5033-5035.

34. Balachandran S, Porosnicu M, Barber GN. Oncolytic activity of vesicular stomatitis virus is effective against tumors exhibiting aberrant p53, Ras, or myc function and involves the induction of apoptosis. J Virol 2001;75: 3474-3479.
35. Kopecky SA, Willingham MC, Lyles DS. Matrix protein and another viral component contribute to induction of apoptosis in cells infected with vesicular stomatitis virus. J Virol 2001;75:12169-12181.
36. Breitbach CJ, Paterson JM, Lemay CG, Falls TJ, McGuire A, Parato KA, et al. Targeted inflammation during oncolytic virus therapy severely compromises tumor blood flow. Mol Ther 2007;15:1686-1693.
37. Zhang H, Wen YJ, Mao BY, Gong QY, Qian ZY, Wei YQ. Plasmid encoding matrix protein of vesicular stomatitis viruses as an antitumor agent inhibiting rat glioma growth in situ. Exp Oncol 2007;29:85-93.
38. Gupta S, Kobayashi S, Phongkitkarun S, Broemeling LD, Kan Z. Effect of transcatheter hepatic arterial embolization on angiogenesis in an animal model. Invest Radiol 2006;41:516-521.
39. Altomonte J, Wu L, Chen L, Meseck M, Ebert O, Garcia-Sastre A, et al. Exponential enhancement of oncolytic vesicular stomatitis virus potency by vector-mediated suppression of inflammatory responses in vivo. Mol Ther 2008;16:146-153.
40. Welsh RM. Regulation of virus infections by natural killer cells. Nat Immun Cell Growth Reg 1986;5:169-199.
41. Nakamoto Y, Mizukoshi E, Tsuji H, Sakai Y, Kitahara M, Arai K, et al. Combined therapy of transcatheter hepatic arterial embolization with intratumoral dendritic cell infusion for hepatocellular carcinoma: clinical safety. Clin Exp Immunol 2007;147:296-305.
42. Takayama T, Sekine T, Makuuchi M, Yamasaki S, Kosuge T, Yamamoto J, et al. Adoptive immunotherapy to lower postsurgical recurrence rates of hepatocellular carcinoma: a randomized trial. Lancet 2000;356:802-807.
43. Diaz R, Galivo F, Kottke T, Wongthida P, Qiao J, Thompson J, et al. Oncolytic immunovirotherapy for melanoma using vesicular stomatitis virus. Cancer Res 2007;67:2840-2848.
44. Di Paolo NC, Tuve S, Ni S, Hellstrom KE, Hellstrom I, Lieber A. Effect of adenovirus-mediated heat shock protein expression and oncolysis in combination with low-dose cyclophosphamide treatment on antitumor immune responses. Cancer Res 2006;66:960-969.
45. Llovet JM, Real MI, Montana X, Planas R, Coll S, Aponte J, et al. Barcelona Liver Cancer Group. Arterial embolisation or chemoembolisation versus symptomatic treatment in patients with unresectable hepatocellular carcinoma: a randomized controlled trial. Lancet 2002; 38:1734-1739.
46. Marelli L, Stigliano R, Triantos C, Senzolo M, Cholongitas E, Davies N, et al. Transarterial therapy for hepatocellular carcinoma: which technique is more effective? A systematic review of cohort and randomized studies. Cardiovasc Intervent Radiol 2006;30:6-25.
47. Petraccia L, Onori P, Sferra R, Lucchetta MC, Liberati G, Grassi M, et al. MDR (multidrug resistance) in hepatocarcinoma clinical-therapeutic implications. Clin Ter 2003;154:325-335.
48. Nies AT, Konig J, Pfannschmidt M, Klar E, Hofmann WJ, Keppler D. Expression of the multidrug resistance proteins MRP2 and MRP3 in human hepatocellular carcinoma. Int J Cancer 2001;94:492-499.
49. Wu XZ, Xie GR, Chen D. Hypoxia and hepatocellular carcinoma: the therapeutic target for hepatocellular carcinoma. J Gastroenterol Hepatol 2007;22:1178-1182.
50. Connor JH, Naczki, Koumenis C, Lyles DS. Replication and cytopathic effect of oncolytic vesicular stomatitis virus in hypoxic tumor cells in vitro and in vivo. J Virol 2004;78:8960-8970.